International Journal of Pharmaceutics 376 (2009) 76–83

Contents lists available at ScienceDirect

International Journal of Pharmaceutics

journal homepage: www.elsevier.com/locate/ijpharm

# A new micro/nanoencapsulated porphyrin formulation for PDT treatment

Daiana K. Deda, Adjaci F. Uchoa, Eduardo Caritá, Maurício S. Baptista, Henrique E. Toma, Koiti Araki*

*Institute of Chemistry, University of Sao Paulo, Av. Prof. Lineu Prestes 748, 05508-000 Sao Paulo, SP, Brazil*

ARTICLE INFO

*Article history:*
Received 2 February 2009
Received in revised form 17 April 2009
Accepted 20 April 2009
Available online 3 May 2009

*Keywords:*
Cationic porphyrin
Polymeric encapsulation
PDT
HeLa cells

ABSTRACT

The highly hydrophobic 5,10,15-triphenyl-20-(3-N-methylpyridinium-yl)porphyrin (3MMe) cationic species was synthesized, characterized and encapsulated in marine atelocollagen/xanthane gum microcapsules by the coacervation method. Further reduction in the capsule size, from several microns down to about 300–400 nm, was carried out successfully by ultrasonic processing in the presence of up to 1.6% Tween 20 surfactant, without affecting the distribution of 3MMe in the oily core. The resulting cream-like product exhibited enhanced photodynamic activity but negligible cytotoxicity towards HeLa cells. The polymeric micro/nanocapsule formulation was found to be about 4 times more phototoxic than the respective phosphatidylcholine lipidic emulsion, demonstrating high potentiality for photodynamic therapy applications.



## 1. Introduction

Photodynamic therapy (PDT) is a medical procedure based on a combined action of a photosensitizer (dye) and light. It has been increasingly employed in the treatment of cancer and other skin diseases, such as psoriasis and vitiligo (leukoderma), with excellent results from medical and aesthetic points of view. Among the several compounds that can be used as dye, porphyrins and derivatives have been extensively employed. In fact, the first commercial phototherapeutic agent called Photofrin®, approved by FDA about 20 years ago, is based on hematoporphyrin oligomers constituted by nine porphyrin units linked by ether, ester and carbon–carbon bonds (Allison et al., 2008; Pushpan et al., 2002; Sharman et al., 1999). Nevertheless, some limitations have been imposed, particularly by the long persistence time in the organism, leading to undesirable skin photosensibility perduring for weeks or even months (Moriwaki et al., 2001; Simplício et al., 2002; Tian et al., 2008). For this reason, more effective and safe photosensitizers and formulations have been pursued (Hopper, 2000; Triesscheijn et al., 2006; Sharman et al., 1999; Bechet et al., 2008; Hudson et al., 2005; Reddi et al., 2002; Kadish et al., 1991; Araki et al., 2000, 2001, 2003; Onuki et al., 1996; Ravanat et al., 1998; Toma and Araki, 2000; Engelmann et al., 2004; Furuta et al., 1994, 1999, 2000, 2003), exhibiting well established chemical composition, high biocompatibility, preferential or specific accumulation in the tumor cells, fast elimination by the organism, high phototoxicity and molar absorptivity in the phototherapeutic window. At the present time only Photofrin®, Levulan® Kerastick and Visudyne® have been approved by FDA for PDT treatment.

*Meso*-tetraarylporphyrins are typical type II photosensitizers. As such their photodynamic action depends on the irradiation with light of suitable wavelength (Dougherty, 1993; Machado, 2000; Pushpan et al., 2002; Simplício et al., 2002; Tian et al., 2008) in the presence of molecular oxygen, because the active species is the singlet oxygen generated by energy transfer from electronically excited dye molecules (Allison et al., 2008; Pushpan et al., 2002; Sharman et al., 1999; Moreira et al., 2008). The action of the very reactive singlet oxygen species is usually confined to the neighborhood where it is generated. Therefore, strategies should be devised to concentrate the photosensitizer as much as possible in the target sites, in order to maximize the photodynamic action and minimize collateral effects. It should be mentioned that the photonecrosis can also be induced indirectly by damaging the peripheral vascular system around the tumor, depriving those cells of nutrients and oxygen (Allison et al., 2008; Simplício et al., 2002).

Although porphyrins and derivatives have interesting photodynamic properties, in general, their solubility in aqueous media is far too low for direct application in PDT treatment. A convenient strategy to increase the biocompatibility and disperse water insoluble lipophilic compounds is the micro- and/or nanoencapsulation in vesicles, liposomes or polymeric capsules. This should be done in such a way that the interior is made lipophilic for allowing the solubilization of non-polar compounds, while their outer side should be hydrophilic making them dispersible in aqueous media.

The polymeric encapsulation represents an interesting choice among the other alternatives, because the capsule shell can be made by several biocompatible polymers and with variable degrees of cross-linking (Reddi, 1997; Torchilin, 2006; Bechet et al., 2008), allowing the control of permeability and mechanical resistance.

* Corresponding author. Tel.: +55 11 3091 8513; fax: +55 11 3815 5579.
*E-mail address:* koiaraki@iq.usp.br (K. Araki).

0378-5173/$ – see front matter © 2009 Elsevier B.V. All rights reserved.
doi:10.1016/j.ijpharm.2009.04.024

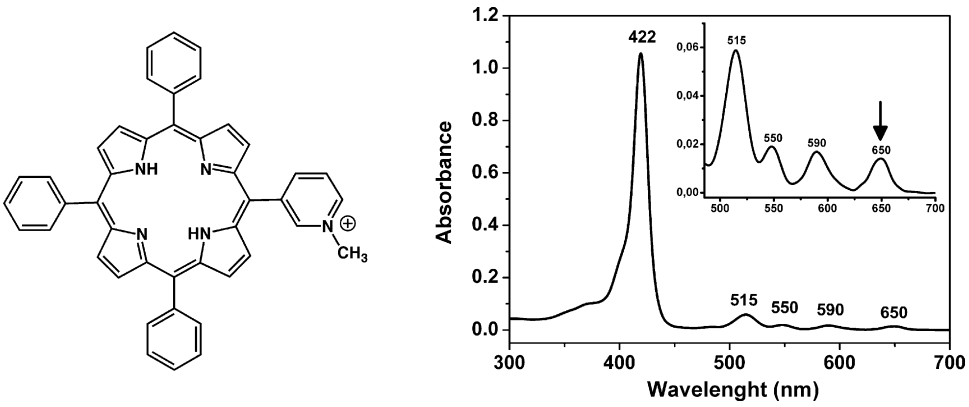


**Fig. 1.** Schematic structure of the 5,10,15-triphenyl-20-(3-N-methylpyridinium-yl)porphyrin, 3MMe, and its absorption spectrum in $CHCl_3$ (right). Inset: expanded view of the spectrum in the visible region.

Polyethyleneglycols are generally added to decrease the interaction between the capsule surface and the plasma components responsible for the activation of the phagocytary cell receptors, minimizing the loss of photosensitizer molecules by opsonization process (Konan et al., 2002; Needhan et al., 1992).

The delivery efficiency (Reddi, 1997; Dong et al., 2007) of micro/nanocapsule formulations is mainly controlled by shell properties (Bamford and Tompa, 1950; Menger and Sykes, 1998) such as chemical composition, morphology, size, mechanical strength and permeability, as well as by the stirring rate, temperature, pressure, pH and even the processing tools employed. Nowadays, several methods such as nebulization, extrusion/solidification, emulsification/solidification, polymerization and coacervation, are available for the preparation of micro- and nanocapsules. The last one, based on a phase separation process, is one of the most commonly used methods for the preparation of polymeric emulsions because of the simplicity and scalability; and was preferred in this work.

Recently we reported on the partition and photodynamic properties of several *meso*-phenyl(pyridinium-yl)porphyrins, and showed that amphiphilic cationic porphyrins interact more effectively with biological membranes, exhibiting enhanced photodynamic activity (Engelmann et al., 2002, 2007a,b). However, the more hydrophobic monocationic species 5,10,15-triphenyl-20-(3-N-methylpyridinium-yl)porphyrin (3MMe, Fig. 1) has not been tested yet because of its rather low solubility in aqueous solution. Now we are overcoming such a problem by using a polymeric micro/nanocapsule formulation. Thus, the preparation, characterization and photodynamic properties of encapsulated 3MMe porphyrin are described in this paper, using HeLa cells as model system.

## 2. Experimental

The 5,10,15-triphenyl-20-(3-N-methylpyridinium-yl)porphyrin, was synthesized and characterized according to the previously described method, as follows (Engelmann et al., 2002, 2007a). A mixture of 53 mmol of benzaldehyde and 18 mmol of 3-pyridyl carboxyaldehyde was reacted with 71 mmol of pyrrol in acetic acid, in the dark. After 2 h, the solvent was removed in a flash evaporator and the porphyrin precipitated-out in a mixture of ethanol and N,N-dimethylformamide 9:1 (v/v). The solid was filtered, washed, dried and purified by column chromatograph in silica-gel using suitable mixtures of $CH_2Cl_2$/EtOH as eluent. The 5,10,15-triphenyl-20-(3-pyridyl)porphyrin was refluxed 4 h with 40 times excess of methyltosylate in N,N-dimethylformamide (DMF), concentrated in a rotary evaporator and poured into a saturated NaCl aqueous solution. The precipitate was separated, redissolved in DMF and reprecipitated in saturated NaCl solution. After repeating this process 3 more times, the 3MMe dye was purified by alumina column chromatography using $CH_2Cl_2$/EtOH mixture as eluent. Analysis: UV–vis spectrum, $\lambda_{max}$ (nm) in $CH_2Cl_2$: 422, 515, 550, 590 and 650. $^1$H NMR (500 MHz, DMSO, TMS): $\delta$ 10.02 (s, 1H), 9.50 (d, 1H), 9.40 (d, 1H), 9.04 (s, 2H), 8.90 (m, 6H), 8.58 (t, 1H), 8.23 (m, 6H), 7.86 (m, 9H), 4.64 (s, 3H), −2.85 (s, 2H).

The 3MMe porphyrin was encapsulated by coacervation according to the following procedure. The 3MMe dye was dissolved in dichloromethane and dispersed in a mixture of isopropylmyristate, almond oil and Tween 20. Then, the resultant suspension was poured into an aqueous xanthane gum suspension, followed by the addition of marine atelocollagen and sodium sulfate (Menger and Sykes, 1998) under vigorous stirring. In this way, a cream-like formulation, stable for months in the refrigerator and containing $1 \times 10^{-4}$ M of the 3MMe dye dissolved in the oily core of polymeric microcapsules, was obtained. This was reprocessed using an ultrasonic tip (VibraCell, from Sonics) in order to get nanocapsules with average size between 100 and 1000 nm. The concentration of Tween 20 in the oil phase was varied from 0.0 to 1.6% in order to evaluate the effect of this surfactant on the size and stability of the capsules.

The encapsulation of the porphyrin was probed by fluorescence spectroscopy in the 600–800 nm interval ($\lambda_{exc}$ = 422 nm), using a Photon Technology Inc., model LS-100 spectrofluorimeter. The micro/nanocapsules were also characterized by fluorescence scanning confocal microscopy using a Zeiss LSM 510 microscope with 100× objective and a 514 nm excitation laser.

The size distribution histograms of the micro- and nanocapsules were obtained by dynamic light scattering measurements using a Microtrac Inc. Nanotrac 252 equipment. Optical microscope images were obtained using a CCD camera with an 100× objective.

The human cervical epithelioid carcinoma cells (HeLa) used in the experiments were cultivated in DMEM culture media, containing 10% of bovine fetal serum and 1% of the antibiotics penicillin and streptomycin, in a Thermo Electron Corporation HEPA class 100 incubator, at 37 °C and atmosphere with 5% of $CO_2$.

The toxicity and phototoxicity of the micro- and nanocapsules formulations were evaluated using HeLa cells. The experiments were carried out by transferring $1 \times 10^5$ cells to each one of the 12 2.0 cm diameter wells of a culture plate and incubating for 15 h for cell adherence. Then, the culture media were removed, 1.0 mL of a 100 times diluted emulsion ([3MMe] = $1 \times 10^{-6}$ M) was added and incubated again, using the same conditions as before. After that, the 3MMe dye emulsion was removed, the wells were carefuly washed with saline PBS solution in order to remove all excess of the formulation and 1 mL of a colorless DMEM culture media was added.

Accordingly, for the phototoxicity experiments, the wells were irradiated with a 630 nm laser (LaserLine, 70 mW cm$^{-2}$) for 10 min,

using an intermitent irradiation mode (1 min on, 1 min off). Then, the plates were incubated for 14 h, the number of viable cells in each well was determined by the methylthiazyldiphenyltetrazolium bromide (MTT) method described below. The control experiment was carried out exactly in the same conditions used for the evaluation of the toxicity and phototoxicity, except for the absence of the encapsulated porphyrin formulation.

The fraction of viable cells was revealed by incubating for 2 h with a 2.0 mg $mL^{-1}$ MTT solution in PBS, and the excess of the green aqueous phase was carefully removed. The formazan crystals, generated by the mitochondrial enzymes present in the viable cells, were dissolved in 1 mL of DMSO and the pink solution analyzed spectrophotometrically at 550 nm, using an Infinite M200 ELISA reader (TECAN). The number of viable cells was estimated from the absorbance measurements considering that they are proportional to the absorbance in the control experiment (100% viability).

The toxicity and phototoxicity of 3MMe porphyrin incorporated in zwiterionic phosphatidylcholine (PC) liposomes were evaluated for comparison purposes. The lipidic formulation was prepared dissolving PC and 3MMe in dichloromethane, evaporating the solvent in a $N_2$ flux and dispersing the film in a colorless DMEM culture media. The emulsion obtained in this way was submitted to ultrasonic processing for 10 min leading to the formation of liposomes with essentially monomodal size distribution and average diameter of 115 nm (Fig. 4, Supplementary Materials). The porphyrin concentration was identical to that in the polymeric micro/nanocapsule emulsion. The toxicity and phototoxicity were evaluated using the same procedure and experimental conditions described above for the micro/nanocapsule formulations.

The amount of 3MMe porphyrin incorporated by the cells was evaluated as a function of the incubation time, using culture plates with adhered HeLa cells (prepared with $2.0 \times 10^5$ cells $mL^{-1}$), and incubated for 1, 2, 3, 4, 6, 7.5 and 9 h. Then, 0.5 mL of the supernatant solution in each well was transferred to separated eppendorf tubes and diluted by adding equal volume of a 50 mM SDS (USB corporation) solution in PBS. The solution remaining in the wells was discarded, the adhered cells washed with small aliquots of PBS and suspended in 0.5 mL of 25 mM SDS in PBS solution. The fluorescence intensity in the 600–800 nm range was measured in a SPEX Fluorolog-2 Fl-111 spectrofluorimeter, using a 10.0 mm quartz cuvette and the front face mode (detection at 45°, $\lambda_{exc}$ = 422 nm). The percentage of porphyrin incorporated in the cells was estimated using Eq. (1):

$$\%\text{incorporation} = 100\frac{F_c}{(F_c + 2F_s)}, \quad (1)$$

where $F_c$ and $F_s$ are the intensities of the porphyrin fluorescence band at 655 nm in the cells and in the supernatant suspension, respectively. $F_s$ is multiplied by a factor of 2 because the solution was diluted to half of its initial concentration, as described above. The plot of fluorescence intensity at 655 nm as a function of porphyrin concentrantion ($1 \times 10^{-9}$ to $1 \times 10^{-6}$ M range) was linear, confirming the validity of the method. The samples were prepared by diluting the porphyrin dye micro/nanocapsule emulsion with colorless DMEM solution.

The results shown in this article are the average of at least three identical experiments performed simultaneously to assure the reproducibily of the experimental conditions.

## 3. Results and discussion

The 3MMe porphyrin exhibits a characteristic Soret band at 422 nm and four Q bands in the 500–700 nm range. The lowest energy band at 650 nm is located within the phototherapeutic window. In spite of the positively charged N-methylpyridinium substituent, the three phenyl groups in the periphery of the porphyrin ring (Fig. 1) impart a strong organophilic character and a high affinity for the cell membrane to the dye molecules (Engelmann et al., 2007a). This is an important characteristic when formulations for topic applications are considered, since ideally, the photosensitizer should stay localized in the region under treatment, avoiding collateral effects caused by unadvised distribution of the dye to the body.

Considering the characteristics of 3MMe dye, we focused on the preparation of a cream-type formulation for topical applications. For this purpose, the micro/nanoencapsulation by the coacervation method is convenient because of the simplicity and the possibility of using a great variety of components, including biocompatible polymers and natural oils commonly used in dermatological formulations. One of these is marine atelocollagen, which was chosen as a capsule wall component because of its high biocompatibility as well as compatibility with the constituents of the outside aqueous environment and the internal oily core of the capsules.

### 3.1. Preparation and characterization of the micro/nanocapsule formulation

The polymeric micro- and nanocapsule emulsions were prepared by pouring the oil phase onto aqueous xanthane gum suspension (1% in weight), under vigorous stirring using a Turrax equipment. Tween 20 was used as one of the components of the oil phase in order to improve the dispersion of the 3MMe porphyrin after removal of the volatile solvent $CH_2Cl_2$ and also to decrease the average size of the polymeric capsules, as described below. Isopropylmyristate was used to adjust the affinity between the oily core and the polymeric capsule. Finally, anhydrous $NaSO_4$ was added to promote the salting-out process, leading to coacervation. As a matter of fact, a sudden increase of ionic strength promotes the dessolvation of the polymer molecules leading to the formation of a capsule layer around the oily core (Menger and Sykes, 1998). At this stage, however, only micrometric capsules are usually formed. Accordingly, further processing is required to get smaller capsules with expected higher penetration capability and photodynamic activity.

The higher shearing force delivered to the system as the stirring rate is increased is known to decrease the average size distribution (Nihant et al., 1995). Accordingly, experiments were carried out, using a polymeric emulsion with no Tween 20 and at increasing rotation rates, but only a small shift in the previous average size distribution was observed by DLS. In fact, no particles smaller than a micron could be observed even after processing at 27,000 rpm. In contrast, a typically bimodal distribution with a significant amount of particles in the 100–1000 nm range was obtained after ultrasonic processing for 10 min, although the majority was still bigger than 1500 nm (Fig. 2a). Accordingly, strategies to improve this method were pursued.

Mayya et al. (2003) showed that small amounts of surfactant can significantly improve the encapsulation efficiency by coacervation method, using microcapsules prepared with gelatin and acacia gum. However, Coffin and Mcginity (1992) reported that polymeric microcapsules containing potassium oleate and sodium dodecylsulfonate (SDS) are more rapidly decomposed than the corresponding formulations with non-ionic pluronic F68 and Tween 20. Such effect was recently attributed to the negative charge acquired by the capsule (Musyanovych et al., 2008). Thus, the effect of the neutral surfactant Tween 20 on the size distribution was verified since the particles size distribution after ultrasonic processing should be influenced by the wall regeneration capability after breakdown of the bigger capsules. As expected, the incorporation of small amounts of Tween 20 (up to 1.6%) led to effective size reduction, as shown in Fig. 2b–f. The fraction of particles with 400–500 nm diameter increased rapidly as a function of Tween 20

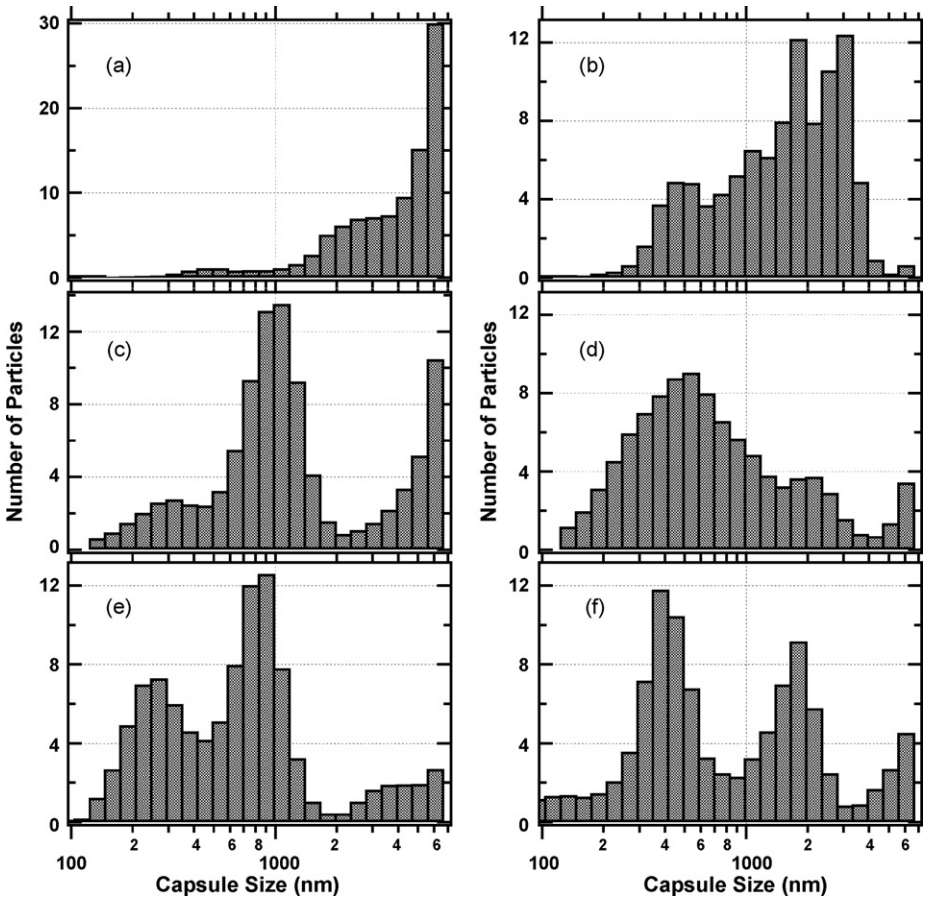


**Fig. 2.** Histograms showing the average size distribution of polymeric capsules in the formulations as a function of the Tween 20 concentration, after 10 min ultrasonic processing: (a) 0%, (b) 0.4%, (c) 0.8%, (d) 1.0%, (e) 1.2% and (f) 1.6%.

concentration reaching the maximum around 1.0%, where a broad almost monomodal distribution was observed. The size histogram for the formulation with 1.2% of Tween 20 (Fig. 2e) showed however a typical bimodal distribution in the 100–2000 nm range, with maxima at 257 nm (37% of the capsules) and 812 nm (51% of the particles), respectively.

Nevertheless, the dynamic light scattering technique is an indirect measurement which is dependent on the inputted parameters, such that a comparison with a direct measurement method might be interesting. Thus, the effect of Tween 20 on the average size distribution of the microcapsules was studied by optical microscopy (Fig. 3). The polymeric formulation without surfactant contains large microcapsules, but the average size is significantly diminished in the formulation with 0.4% of Tween 20, where only microcapsules smaller than about 10 μm in diameter are visible (Fig. 3b). Interestingly, the amount of capsules seems to decrease when the surfactant concentration was doubled, indicating that the majority of them are now below the optical resolution of the microscope. In fact, only few microcapsules are visible in the polymeric formulations with 1.0–1.2% of Tween 20, as shown in Fig. 3d and e, but the amount increased again significantly when the concentration of surfactant was enhanced further to 1.6% (Fig. 3f), corroborating the DLS results (Fig. 2f). Thus, Tween 20 seems to favor both, the breakdown and formation of smaller capsules at lower concentrations but also the coalescence processes at higher concentrations (above 1.0–1.2%).

Another important aspect to be considered is the actual distribution of the 3MMe porphyrin in the capsules. Considering that the coacervation process was carried out successfully, the photosensitizer should be dispersed in the oily core. However, it also can be incorporated in the capsule walls or attached to the outer surface. Confocal fluorescence microscopy is a convenient tool for this purpose, as shown in Fig. 4. The images were obtained using samples that were not submitted to ultrasonic processing and focusing on the bigger particles for better visualization. In the fluorescence mode image (Fig. 4b), the red light emitting porphyrin dye appears uniformly distributed forming round shaped droplets. Furthermore, the walls are clearly visible in the images obtained using the combined transmission/fluorescence mode (arrows in Fig. 4a). A more careful analysis showed that there is a perfect superimposition between the positions of the capsules determined by conventional optical microscopy and those obtained by confocal fluorescence microscopy, thus confirming that the porphyrin molecules are inside the capsules. Most of the capsules appear blurred because they are not in the microscope focus.

### *3.2. Toxicity and phototoxicity of the micro/nanocapsule formulation*

Considering the results describe above, the formulation containing 1.2% of Tween 20 was chosen for the toxicity and phototoxicity experiments. In the toxicity tests, $1 \times 10^5$ HeLa cells were incubated for 3 h without and with the polymeric micro/nanocapsules ([3MMe] = $1 \times 10^{-6}$ M), and compared with the control. In order to evaluate the phototoxicity of the capsules loaded or not with the porphyrin photosensitizer, the samples were irradiated with a red laser ($\lambda$ = 630 nm, 70 mW cm$^{-2}$) for 10 min. No change in the number of viable cells was observed (Fig. 5) in the experiments using the formulation without the 3MMe porphyrin dye (exp. C), but decreased 60% in the experiments using the formulation

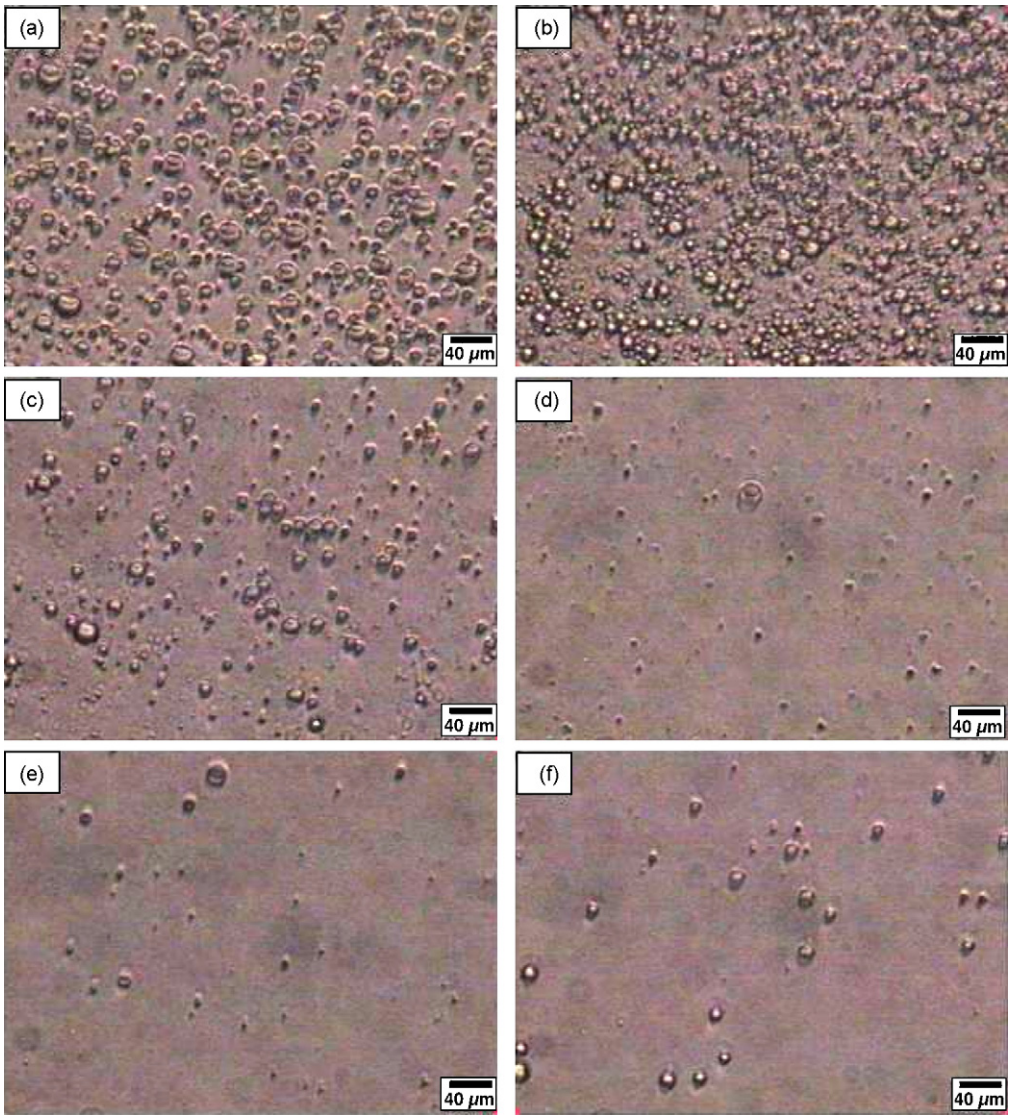


**Fig. 3.** Optical microscopy images (900× magnification) of the microcapsule formulations prepared and processed in the same way as in Fig. 2: (a) 0.0%, (b) 0.4%, (c) 0.8%, (d) 1.0%, (e) 1.2% and (f) 1.6% of Tween 20.

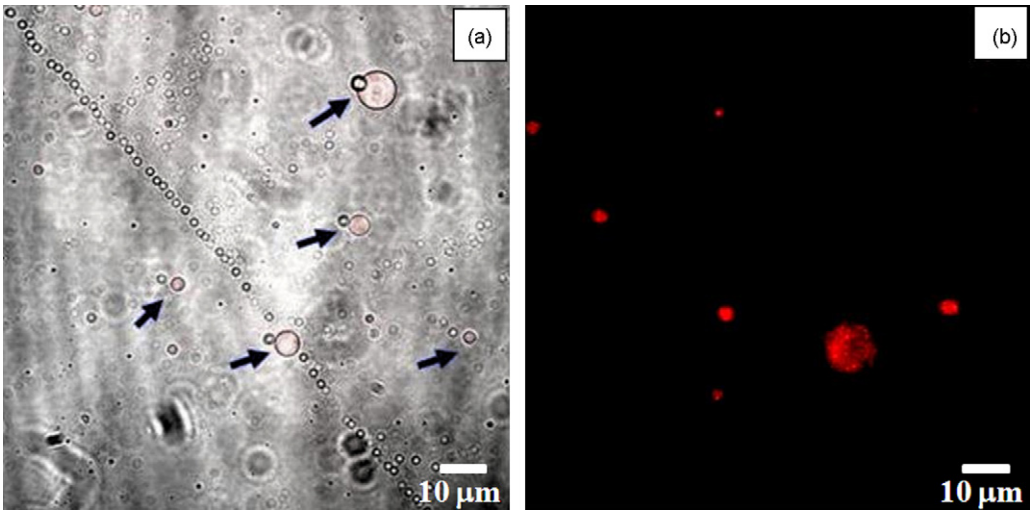


**Fig. 4.** Confocal fluorescence microscopy images of polymeric microcapsules containing $1.0 \times 10^{-4}$ M of 3MMe in combined transmission/fluorescence (a) and fluorescence (b) modes, using excitation laser of $\lambda_{exc} = 514$ nm. The arrows indicate the capsules (in the microscope focus) in which it is possible to see that the images obtained by fluorescence and optical microscopy are matching.

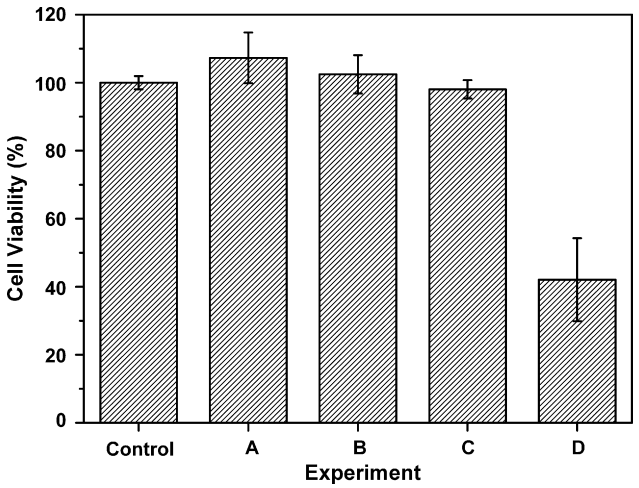


**Fig. 5.** Percentage of viable HeLa cells after incubation for 3 h, in the absence (control) and presence of polymeric micro/nanocapsule emulsion without (A) and loaded with $1 \times 10^{-6}$ M 3MMe (B) in the dark and (C and D, respectively) irradiated for 10 min with 630 nm, 70 mW cm$^{-2}$ laser.

containing the porphyrin photosensitizer (Fig. 5 exp. D). This result is very significant confirming that the toxicity of the particles alone (Fig. 5, exp. A) and loaded with the photosensitizer (Fig. 5, exp. B) is negligible in the dark, and the phototoxicity (Fig. 5, exp. C) of the polymeric capsules alone was shown to be negligible also. Consequently, the porphyrin molecules delivered to the cells should be the only responsible for the photodynamic activity.

Several factors such as molar absorptivity, photochemical activity of the photosensitizer in the excited state, mechanism of photodynamic action, and affinity for the tissues and cell membrane, can influence the phototoxicity. All of them are intrinsic properties of the dye and should be optimized by molecular engineering. The light dose is another factor that influence the phototoxicity because the damage must be high enough to induce apoptosis or necrosis of the cells. Accordingly, a study was carried out using the same conditions adopted for the experiments described in Fig. 5 but varying the irradiation time. No significant cell death was observed until about 3 min, but the number of viable cells was reduced to 20 and 50% when the exposition time was increased to 5 and 10 min, respectively, as shown in Fig. 6a.

Another important factor is the incubation time, that should reflect on the amount of 3MMe photosensitizer delivered to the cells. In fact, a dramatic effect of the incubation time on the cell viability was found (Fig. 6b) in the experiments carried keeping all other parameters constant. In fact, the fraction of dead cells increased steadily reaching more than 80% for the samples incubated for 9 h and irradiation time as short as 10 min.

Such a remarkable effect should be related with the amount of porphyrin delivered to the HeLa cells. In order to evaluate this important aspect, the fraction of incorporated 3MMe dye molecules was determined by fluorescence spectrometry (Fig. 7a), as follows. Initially, samples were prepared diluting the concentrated polymeric micro/nanocapsule emulsion with colorless DMEM culture media and the respective emission spectra were registered. An excellent linear correlation ($R = 0.9998$) was found for the plot of the fluorescence intensity at 655 nm as a fuction of 3MMe dye concentration ($1 \times 10^{-9}$ to $1 \times 10^{-6}$ M range, Fig. 7b), indicating that fluorescence measurements are suitable for the determination of porphyrin concentration in the supernatant. Interestingly, the fraction of 3MMe molecules incorporated in the HeLa cells (calculated using Eq. (1)) is also a linear function of the incubation time

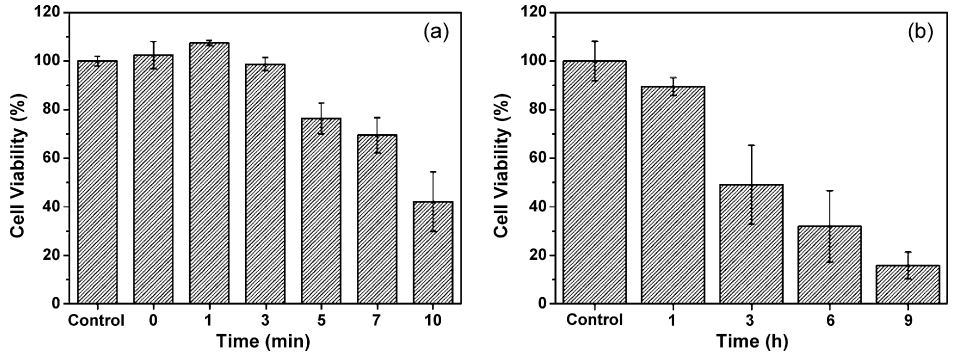


**Fig. 6.** Influence of the (a) irradiation time and (b) incubation time on the phototoxicity of polymeric micro/nanocapsule 3MMe emulsion. The experimental conditions are identical to that in Fig. 5, except for the irradiation time.

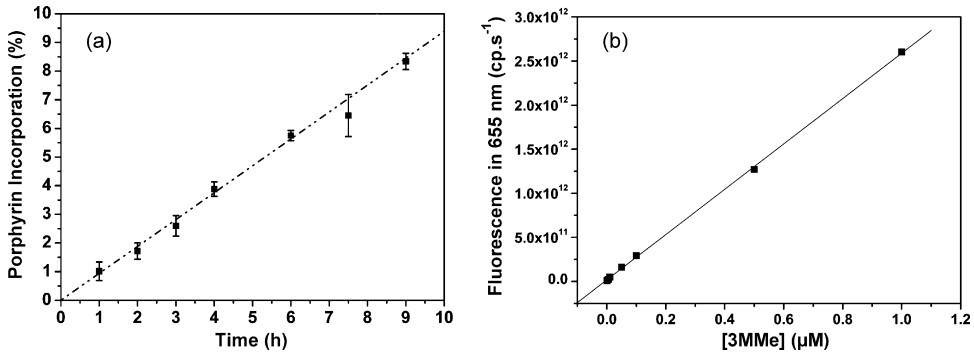


**Fig. 7.** (a) Fraction of 3MMe molecules incorporated by HeLa cells ($2.0 \times 10^5$ cells mL$^{-1}$) as a function of the incubation time in the presence of polymeric micro/nanoencapsulated formulation (3MMe) = $1 \times 10^{-6}$ M. (b) Plot of the fluorescence intensity at 655 nm as a function of 3MMe concentration ($1 \times 10^{-9}$ to $1 \times 10^{-6}$ M range), $\lambda_{exc}$ = 422 nm. The samples were diluted with colorless DMEM culture media.

($R$ = 0.998, Fig. 7a), while the cell viability decreased exponentially as a function of the incubation time (Fig. 6b and Supplementary Materials, Fig. 3). Accordingly, the cell viability should be a function of the amount of incorporated porphyrin photosensitizer also, thus explaining the increase of the photodynamic efficiency as a function of the incubation time.

One could argue that the observed photodynamic efficiency might be due to the cytotoxicity of the porphyrin formulation itself at longer times. To clarify this point, experiments were carried out measuring the cell viability in the same conditions as described for those in Fig. 6b, but in the dark. In this case, no change was observed in the cell viability (Supplementary Materials, Fig. 1) even after 9 h of incubation in the presence of the polymeric micro/nanocapsule formulation.

It is well known, however, that liposomal emulsions have been successfully employed for the development of products based on lipophilic water insoluble pharmaceutics (Cevc, 2004; Konan et al., 2002; Xiang and Anderson, 2006). They are known to have high affinity for the membrane and efficiently deliver their content to cells (Ikeda et al., 2007). For this reason, the toxicity and phototoxicity of 3MMe porphyrin loaded polymeric micro/nanocapsule formulation were compared with those of an equivalent lipidic formulation prepared with zwitterionic lipide, phospatidylcolline (PC). The average concentration of the porphyrin photosensitizer is equivalent in both formulations, such that their properties can be directly compared. The lipidic emulsion exhibited bimodal size distribution with the majority of the particles with mean diameter equal to 115 nm and about 10% with 400 nm, as shown in Supplementary Materials (Fig. 4). The fluorescence spectra of the lipidic and polymeric micro/nanocapsule emulsion exhibited similar profiles, but 50% much higher intensity. This suggests that the porphyrin molecules are interacting more extensively in the polymeric capsules (see Supplementary Materials, Fig. 3), but this formulation was found to be about 4 times more phototoxic than the lipidic formulation (Fig. 8, exps. D and C, respectively). Since both showed negligible cytotoxicity (Fig. 8, exps. A and B) in the dark, the main factor responsible for the enhanced photodynamic activity should be the more effective interaction and higher capability of the nano/microcapsules to deliver the porphyrin dye content to the HeLa cells. In fact, the relationship between the efficiency of photosensizitizer incorporation process, membrane binding and PDT activity has been demonstrated using several model systems (Engelmann et al., 2007a,b; Pavani et al., 2009).

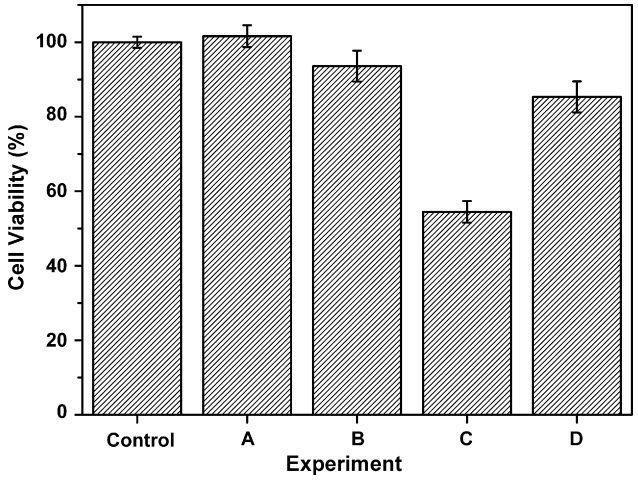


**Fig. 8.** Toxicity of the polymeric micro/nanocapsule (A) and phosphatidylcolline (B) 3MMe emulsion towards HeLa cells ($1 \times 10^5$ cells mL$^{-1}$) in the dark; and when irradiated for 10 min with 70 mW cm$^{-2}$, 630 nm laser (C and D, respectively).

## 4. Final remarks

A new cream-like polymeric emulsion containing 3MMe porphyrin dispersed in almond oil and encapsulated in marine atelocollagen/xanthane gum micro/nanocapsules was prepared by the coacervation method. The incorporation of the neutral surfactant Tween 20 combined with ultrasonic processing was shown to be very effective in the reduction of the capsule size from several microns to about 300–400 nm. The porphyrin is uniformly dispersed in the oily core of the polymeric micro/nanocapsules and the formulation was about 4 times more phototoxic towards HeLa cells than a liposomal emulsion of zwitterionic phosphatidylcholine loaded with an equivalent amount of the porphyrin. In fact, more than 80% of the cells were inactivated after 10 min irradiation with a 630 nm laser, but no change was found in the dark. Thus, the proposed 3MMe micro/nanocapsule formulation does provide a promising alternative for application in PDT treatment.

## Acknowledgements

We gratefully acknowledge the financial support and fellowship from the Brazilian agencies, Fundação de Amparo à Pesquisa do Estado de São Paulo (FAPESP) and Conselho Nacional de Desenvolvimento Científico e Tecnológico (CNPq); and Instituto do Milênio de Materiais Complexos.

## Appendix A. Supplementary data

Supplementary data associated with this article can be found, in the online version, at doi:10.1016/j.ijpharm.2009.04.024.

## References

Allison, R.R., Mota, H.C., Bagnato, V.S., Sibata, C.H., 2008. Bio-nanotechnology and photodynamic therapy state of the art review. Photodiagn. Photodyn. Ther. 5, 19–28.
Araki, K., Engelmann, F.M., Mayer, I., Toma, H.E., Baptista, M.S., Maeda, H., Osuka, A., Furuta, H., 2003. Doubly N-confused porphyrins as efficient sensitizers for singlet oxygen generation. Chem. Lett. 32, 244–245.
Araki, K., Silva, C.A., Toma, H.E., Catalani, L.H., Medeiros, M.H.G., Mascio, P.D., 2000. Zinc tetraruthenated porphyrin binding and photoinduced oxidation of calf-thymus DNA. J. Inorg. Biochem. 78, 269–273.
Araki, K., Winnischofer, H., Toma, H.E., Maeda, H., Osuka, A., Furuta, H., 2001. Acid–base and spectroelectrochemical properties of doubly N-confused porphyrins. Inorg. Chem. 40, 2020–2025.
Bamford, C.H., Tompa, H., 1950. The theory of coacervation. Trans., Faraday Soc. 46, 310–316.
Bechet, D., Couleaud, P., Frochot, C., Viriot, M.L., Guillemin, F., Barberi-Heyob, M., 2008. Nanoparticles as vehicles for delivery of photodynamic therapy agents. Trends Biotechnol. 26, 612–621.
Cevc, G., 2004. Lipid vesicles and other colloids as drug carriers on the skin. Adv. Drug Deliv. Rev. 56, 675–711.
Coffin, M.D., Mcginity, J.W., 1992. Biodegradable pseudolatexes—the chemical-stability of poly(D,L-lactide) and poly (epsilon-caprolactone) nanoparticles in aqueous-media. Pharm. Res. 9, 200–205.
Dong, Z.J., Toure, A., Jia, C.S., Zhang, X.M., Xu, S.Y., 2007. Effect of processing parameters on the formation of spherical multinuclear microcapsules encapsulating peppermint oil by coacervation. J. Microencapsul. 24, 634–646.
Dougherty, T.J., 1993. Photodynamic therapy. Photochem. Photobiol. 58, 895–900.
Engelmann, F.M., Mayer, I., Araki, K., Toma, H.E., Baptista, M.S., Maeda, H., Osuka, A., Furuta, H., 2004. Photochemistry of doubly N-confused porphyrin bonded to non-conventional high oxidation state Ag(III) and Cu(III) ions. J. Photochem. Photobiol. A 163, 403–411.
Engelmann, F.M., Mayer, I., Gabrielli, D.S., Toma, H.E., Kowaltowski, A.J., Araki, K., Baptista, M.S., 2007a. Interaction of cationic meso-porphyrins with liposomes, mitochondria and erythrocytes. J. Bioenerg. Biomembr. 39, 175–185.
Engelmann, F.M., Rocha, S.V.O., Toma, H.E., Araki, K., Baptista, M.S., 2007b. Determination of n-octanol/water partition and membrane binding of cationic porphyrins. Int. J. Pharm. 329, 12–18.
Engelmann, F.M., Winnischofer, H., Araki, K., Toma, H.E., 2002. Synthesis, electrochemistry, spectroscopy and photophysical properties of a series of meso-phenylpyridylporphyrins with one to four pyridyl rings coordinated to [Ru(bipy)2Cl]+ groups. J. Porphyrins Phthalocyanines 6, 33–42.
Furuta, H., Asano, T., Ogawa, T., 1994. N-confused porphyrin—a new isomer of tetraphenylporphyrin. J. Am. Chem. Soc. 116, 767–768.

Furuta, H., Ishizuka, T., Osuka, A., Ogawa, T., 2000. N-fused porphyrin: a new tetrapyrrolic porphyrinoid with a fused tri-pentacyclic ring. J. Am. Chem. Soc. 122, 5748–5757.
Furuta, H., Morimoto, T., Osuka, A., 2003. Syntheses, structures, and crystal packing of N-confused 5,20-diphenylporphyrin and Ag(III) complex. Org. Lett. 5, 1427–1430.
Furuta, H., Ogawa, T., Uwatoko, Y., Araki, K., 1999. N-confused tetraphenylporphyrin–silver(III) complex. Inorg. Chem. 38, 2676–2682.
Hopper, C., 2000. Photodynamic therapy: a clinical reality in the treatment of cancer. Lancet Oncol. 1, 212–219.
Hudson, R., Savoie, H., Boyle, R.W., 2005. Lipophilic cationic porphyrins as photodynamic sensitzers. Photodiagn. Photodyn. Ther. 2, 193–196.
Ikeda, A., Doi, Y., Nishiguchi, K., Kitamura, K., Hashizume, M., Kikuchi, J.I., Yogo, K., Ogawa, T., TakeyaA, T., 2007. Induction of cell death by photodynamic therapy with water-soluble lipid-membrane-incorporated [60]fullerene. Org. Biomol. Chem. 5, 1158–1160.
Kadish, K.M., Maiya, B.G., Araullomcadams, C., 1991. Spectroscopic characterization of meso-tetrakis(1-methylpyridinium-4-yl)porphyrins, [(Tmpyp)H2]4+ and [(Tmpyp)M]4+, in aqueous micellar media, where M = $Vo^{2+}$, Cu(Ii), and Zn(Ii). J. Phys. Chem. 95, 427–431.
Konan, Y.N., Gurny, R., Allemann, E., 2002. State of the art in the delivery of photosensitizers for photodynamic therapy. J. Photochem. Photobiol. B 66, 89–106.
Machado, A.E.D.H., 2000. Terapia fotodinâmica: princípios, potencial de aplicação e perspectivas. Quim. Nova 23, 237–243.
Mayya, K.S., Bhattacharyya, A., Argillier, J.F., 2003. Micro-encapsulation by complex coacervation: influence of surfactant. Polym. Int. 52, 644–647.
Menger, F.M., Sykes, B.M., 1998. Anatomy of a coacervate. Langmuir 14, 4131–4137.
Moreira, L.M., Dos Santos, F.V., Lyon, J.P., Maftoum-Costa, M., Pacheco-Soares, C., Da Silva, N.S., 2008. Photodynamic therapy: porphyrins and phthalocyanines as photosensitizers. Aust. J. Chem. 61, 741–754.
Moriwaki, S.I., Misawa, J., Yoshinari, Y., Yamada, I., Takigawa, M., Tokura, Y., 2001. Analysis of photosensitivity in Japanese cancer-bearing patients receiving photodynamic therapy with porfimer sodium (Photofrin (TM)). Photodermatol. Photoimmunol. Photomed. 17, 241–243.
Musyanovych, A., Schmitz-Wienke, J., Mailander, V., Walther, P., Landfester, K., 2008. Preparation of biodegradable polymer nanoparticles by miniemulsion technique and their cell interactions. Macromol. Biosci. 8, 127–139.
Needhan, D., Mcintosh, T.J., Lasic, D.D., 1992. Repulsive interactions and mechanical stability of polymer-grafted lipid membranes. Biochim. Biophys. Acta 1108, 40–48.
Nihant, N., Grandfils, C., Jerome, R., Teyssie, P., 1995. Microencapsulation by coacervation of poly(lactide-co-glycolide): 4. Effect of the processing parameters on coacervation and encapsulation. J. Controlled Release 35, 117–125.
Onuki, J., Ribas, A.V., Medeiros, M.H.G., Araki, K., Toma, H.E., Catalani, L.H., Di Mascio, P., 1996. Supramolecular cationic tetraruthenated porphyrin induces single-strand breaks and 8-oxo-7,8-dihydro-2′-deoxyguanosine formation in DNA in the presence of light. Photochem. Photobiol. 63, 272–277.
Pavani, C., Uchoa, A.F., Oliveira, C.S., Iamamoto, Y., Baptista, M.S., 2009. Effect of zinc insertion and hydrophobicity on the membrane interactions and PDT activity of porphyrin photosensitizers. Photochem. Photobiol. Sci. 8, 233–240.
Pushpan, S.K., Venkatraman, S., Anand, V.G., Sankar, J., Parmeswaran, D., Ganesan, S., Chandrashekar, T.K., 2002. Porphyrins in photodynamic therapy—a search for ideal photosensitizers. Curr. Med. Chem. - Anti-Cancer Agents 2, 187–207.
Ravanat, J.L., Cadet, J., Araki, K., Toma, H.E., Medeiros, M.H.G., Di Mascio, P., 1998. Supramolecular cationic tetraruthenated porphyrin and light-induced decomposition of 2′-deoxyguanosine predominantly via a singlet oxygen-mediated mechanism. Photochem. Photobiol. 68, 698–702.
Reddi, E., 1997. Role of delivery vehicles for photosensitizers in the photodynamic therapy of tumours. J. Photochem. Photobiol. B 37, 189–195.
Reddi, E., Ceccon, M., Valduga, G., Jori, G., Bommer, J.C., Elisei, F., Latterini, L., Mazzucato, U., 2002. Photophysical properties and antibacterial activity of meso-porphyrin. Photochem. Photobiol. 75, 462–470.
Sharman, W.M., Allen, C.M., Van Lier, J.E., 1999. Photodynamic therapeutics: basic principles and clinical applications. D.D.T. 4, 507–517.
Simplício, F.I., Maionchi, F., Hioka, N., 2002. Terapia Fotodinâmica: aspectos farmacológicos, aplicações e avanços recentes no desenvolvimento de medicamentos. Quim. Nova 25, 801–807.
Tian, Y.Y., Wang, L.L., Wang, W., 2008. Progress in photodynamic therapy on tumors. Laser Phys. 18, 1119–1123.
Toma, H.E., Araki, K., 2000. Supramolecular assemblies of ruthenium complexes and porphyrins. Coord. Chem. Rev. 196, 307–329.
Torchilin, V.P., 2006. Multifunctional nanocarriers. Adv. Drug Deliv. Rev. 58, 1532–1555.
Triesscheijn, M., Baas, P., Schellens, J.H.M., Stewart, F.A., 2006. Photodynamic therapy in oncology. The Oncologist 11, 1034–1044.
Xiang, T.X., Anderson, B.D., 2006. Liposomal drug transport: a molecular perspective from molecular dynamics simulations in lipid bilayers. Adv. Drug Deliv. Rev. 58, 1357–1378.